ROYAL SOCIETY
OF CHEMISTRY

PAPER

Check for updates

Flexible polyolefin dielectric by strategic design of organic modules for harsh condition electrification†

Ajinkya A. Deshmukh, [iD] ‡[a] Chao Wu,‡[b] Omer Yassin,[c] Ankit Mishra,[d]
Lihua Chen, [iD] [e] Abdullah Alamri, [iD] [a] Zongze Li,[bf] Jierui Zhou,[bf] Zeynep Mutlu,[g]
Michael Sotzing,[b] Pankaj Rajak,[d] Stuti Shukla,[c] John Vellek,[c]
Mohamadreza Arab Baferani,[b] Mukerrem Cakmak, [iD] [g] Priya Vashishta,[d]
Rampi Ramprasad,[e] Yang Cao [iD] ★[bf] and Gregory Sotzing★[ac]

Flexible polymers that can withstand temperature and electric field extremes are critical to advanced electrical and electronic systems. High thermal stability of polymers is generally achieved through the introduction of highly conjugated aromatic structures, that lower the bandgap and thus diminish the electric field endurance. Here, we demonstrate a class of flexible all-organic polyolefins by a strategic modular structure design to eliminate the impact of conjugation on bandgap. The one such designed polymer exhibits superior operational temperature and T_g of 244 °C without compromising the bandgap (∼5 eV), exhibiting significantly suppressed electrical conductivity when subjected to a high electric field. It reveals the highest ever recorded energy density of 6.5 J cc^{-1} at 200 °C, a 2× improvement over the best reported flexible dielectric polymers or polymer composites. The uncovered polymer design strategy introduces a platform for high performance dielectric development for extreme thermal and electric field conditions.

Broader context

Continuous improvement in flexible polymer dielectrics is indispensable for constantly advancing and miniaturizing electrical devices. For capacitive energy storage devices, polymer dielectrics withstanding extreme thermal and electrical conditions are necessary to achieve high energy density and payload efficiency for harsh condition electrifications. However, traditional high-temperature polymer dielectrics all have inherent limitations in that their aromatic backbones lead to diminishing bandgap and hence high loss and low breakdown strength, especially at high temperatures. In this work, we use the molecular engineering approach to eliminate the design constrain and report an all-organic polymer that exhibits a large bandgap of ∼5 eV while with also high thermal stability (T_g ∼ 244 °C), resulting in a record high energy density of 6.5 J cc^{-1} at an elevated temperature of 200 °C. This work uncovers a new approach in the design of flexible and scalable dielectric materials with high energy density and, most importantly, high discharge efficiency at elevated temperatures, broadly applicable for electric propulsions, avionics, renewable integration and high-density microelectronics.

[a] *Institute of Materials Science, University of Connecticut, Storrs, CT 06269, USA.*
E-mail: g.sotzing@uconn.edu
[b] *Electrical Insulation Research Center, Institute of Materials Science, University of Connecticut, Storrs, CT 06269, USA. E-mail: yang.cao@uconn.edu*
[c] *Department of Chemistry, University of Connecticut, Storrs, CT 06269, USA*
[d] *Collaboratory for Advanced Computing and Simulations, Department of Chemical Engineering and Materials Science, Department of Physics & Astronomy, and Department of Computer Science, University of Southern California, Los Angeles, CA 90089, USA*
[e] *School of Materials Science and Engineering, Georgia Institute of Technology, Atlanta, GA 30332, USA*
[f] *Department of Electrical and Computer Engineering, University of Connecticut, Storrs, CT 06269, USA*
[g] *School of Materials Engineering, Purdue University, West Lafayette, IN 47907, USA*
† Electronic supplementary information (ESI) available. See DOI: 10.1039/d1ee02630e
‡ These authors contributed equally to this work.

The role of polymers in electronic and electrical devices is significant due to their tunable electrically insulating or conducting properties, flexibility and ease of processing.[1–11] In particular, dielectric polymers resistant to high electric fields are widely used for capacitive energy storage devices, power cables and as gate dielectrics for organic field-effect transistors, *etc.*[4,7,12–14] Polyolefins such as polyethylene (PE) and polypropylene (PP) are generally used for high electric field applications due to their low conduction loss which is ascribed to having a large bandgap.[7] For applications such as space exploration, oil and gas lodging instruments, high performance motors, electric vehicles, and for future passenger aircrafts, hybrid electrification systems are exposed to elevated

This journal is © The Royal Society of Chemistry 2022

Energy Environ. Sci., 2022, **15**, 1307–1314 | **1307**

temperatures in excess of 200 °C during operation.[15–18] Conventional polymers with high electric field endurance have a low glass transition temperature (T_g) or melting temperature (T_m) resulting in low operating temperatures due to changes in electrical characteristics when the temperature is above these second order or first order phase change thermal transitions. For example, PE and biaxially oriented PP (BOPP) must be used below 100 °C. On the other hand, present high-temperature polymers show noticeable electrical conduction at ambient and elevated temperatures, giving rise to deteriorated electric field endurance and increased energy loss.[6,19] Therefore, there is an immense gap between molecular engineering of polymers that have high thermal stability and polymers that have high electric field stability.

Bandgap is the foremost parameter for determining high electric field endurance. It is a measure of the energy required for an electron to travel from the valence band to the conduction band, which determines the electrical conduction of polymers.[20] The T_g is an established gauge parameter for polymer thermal stability. High T_g is necessary for polymers to operate at an elevated temperature, as polymers with T_g close to the operating temperature lose their mechanical integrity, leading to increased electrical conduction. The high T_g and thermal stability of conventional high temperature polymers is improved by incorporating a large number of conjugated aromatic groups in the polymer backbone. These aromatic groups lower the bandgap, giving rise to prominent electrical conduction at high electric fields (Fig. 1a). Polymers that have a superior high-electric-field endurance are composed of an aliphatic polymer backbone. The absence of any aromatic moieties in the polymer backbone results in a large bandgap, as there is no conjugation or pi-pi stacking available. Poor thermal stability for conventional dielectric polyolefins can be attributed to less substantial molecular forces between polymer chains as well as the lack of rigidity in the backbone limiting their usage at elevated temperatures (Fig. 1a). As a result, an inverse correlation between T_g and bandgap for conventional high temperature polymers has been reported.[6] To break the constraint of the aforementioned T_g and bandgap, great efforts have been made to suppress the electrical conduction of high temperature polymers by using external components, usually by making composites or coating established high-temperature polymers with large bandgap inorganic materials. Though there is appreciable suppression in the electrical conduction, this approach of extrinsically improving the bandgap faces issues in flexibility, processability, cost and performance at high electric fields.[21–23] Compromising flexibility and processability are not desirable, as these parameters are important for real-life applications.[24] Therefore, there is an urgent need for flexible, processable all-organic polymers that have intrinsically high electric field and high temperature stability simultaneously.

We have developed a modular polymer design strategy through which high temperature stability and large bandgaps are achieved simultaneously. Rigid bicyclic aliphatics are present in the polymer backbone to reduce the conjugation length

as well as to minimize the pi–pi stacking to achieve a large bandgap while maintaining the high temperature stability. To improve thermal stability, aromatic groups are incorporated as side groups rather than into the backbone of the polymer. The presence of rigid bicyclics in the backbone along with an aromatic side group elevates T_g without compromising bandgap. The schematics of the polymer structures developed using this strategy are shown in Fig. 1a and b. A class of polymers, Polyoxafluorinatednorbornene (POFNB) prepared by the versatile ring opening metathesis polymerization (ROMP), is designed by changing the –CF$_3$ substitution position on the benzene ring to optimize the electrical and thermal properties (Fig. S1–S9, ESI†).

The resulting set of polymers do not follow the inverse T_g vs bandgap trend, unlike other high temperature polymers (Fig. 1c and Fig. S11–S18, S21–S23, ESI†). Furthermore, the large bandgap of these polymers was confirmed by the electronic density of states (DOS) computed using density functional theory (Fig. 1d). The bandgap derived from the DOS for several polymers reveals the advantages of the polymer design strategy in this work. In particular, *ortho*-Polyoxafluorinatednorbornene (*o*-POFNB) shows the largest bandgap (~ 5 eV) and highest T_g of 244 °C among all POFNBs.

When subjected to a high electric field, polymers exhibit a nonlinear increase in electrical conduction due to the carrier injection, excitation, and transport, an effect which is exacerbated at elevated temperatures.[6,25,26] This increase in high field conduction is observed even at temperatures well below T_g. The dramatically increased electrical conduction gives rise to substantial enhancement of the energy loss for energy storage devices, significant promotion of the leakage current for gate dielectrics of organic field effect transistors and strong distortion of electric field for high voltage power cable insulation. The high field conduction of *o*-POFNB, which has the largest bandgap among polymers with a $T_g > 100$ °C, along with other established commercially available dielectric polymers were investigated using a test system which can dynamically cancel the capacitive component and probe the resistive conduction current down to 10 ppm during the voltage ramp all the way to breakdown (Fig. 2). From the integral conduction current (ICC) it can be seen that at room temperature (RT) the ICC of PI is the highest among all high temperature polymers investigated owing to the lowest bandgap. Although BOPP has the lowest ICC at room temperature due to its largest bandgap, at 100 °C the ICC of BOPP is slightly higher than POFNB and *o*-POFNB due to the low T_g of BOPP. At 100 °C, the upper limit of the operational temperature for density polyethylene (HDPE), HDPE exhibits the highest ICC due to the degraded thermal stability. At 150 °C, *o*-POFNB shows the lowest ICC relative to other high temperature polymers. The high T_g of *o*-POFNB (244 °C) compared to POFNB (186 °C) plays an important role in the electrical conduction at such a high temperature (150 °C). At 150 °C, approaching the T_g of POFNB (186 °C), the segmental movement of polymer chains under extremely high electric field possibly contributes to the higher conduction of POFNB than that of *o*-POFNB. With smaller bandgaps, the

1308 | *Energy Environ. Sci.*, 2022, **15**, 1307–1314
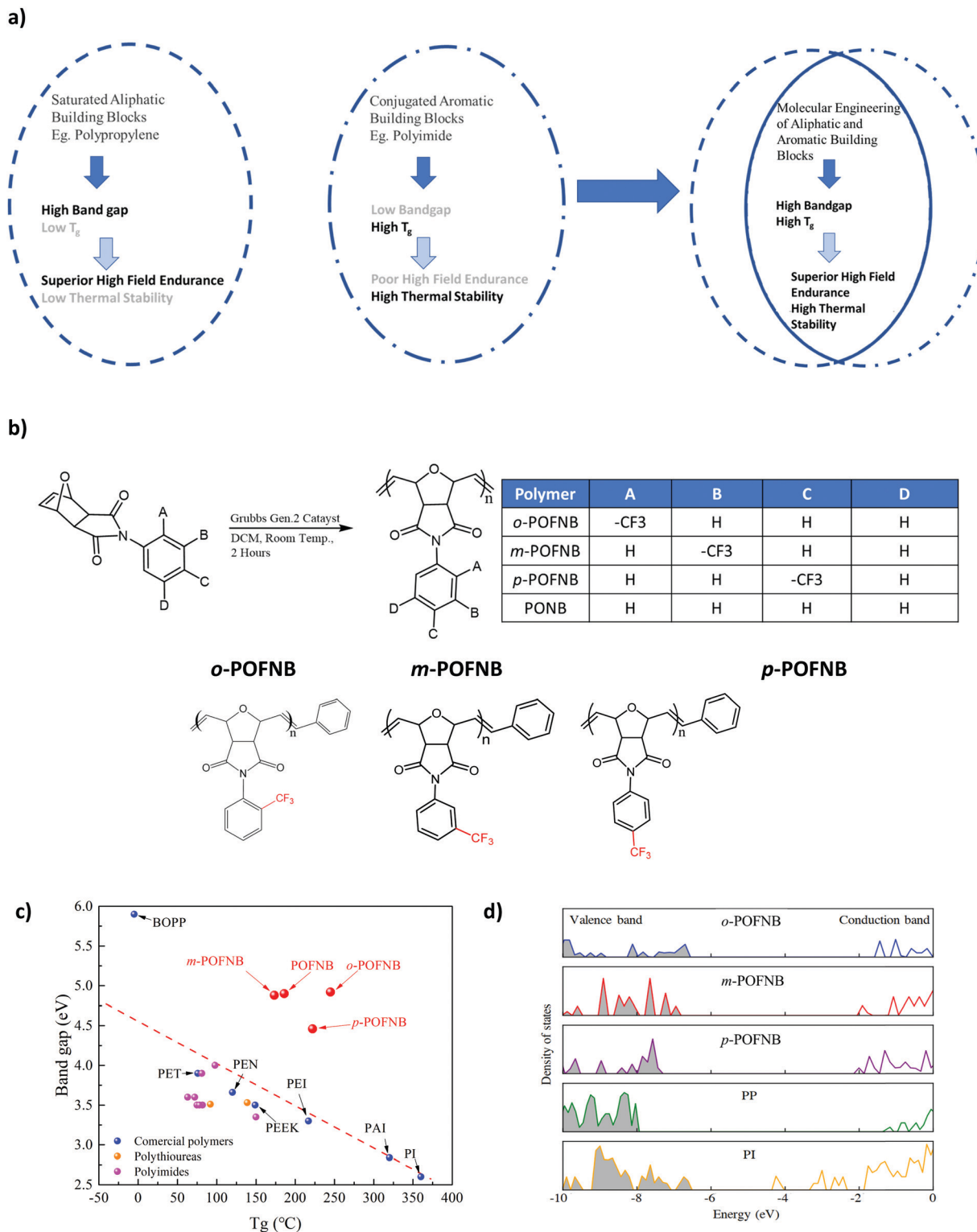
This journal is © The Royal Society of Chemistry 2022

Fig. 1 Design of High Temperature Polymer Dielectrics. (a) Conceptual schematic for design of high temperature dielectric polymers. (b) Molecular structures of polymers investigated in this work. (c) The bandgap *vs.* T_g for polymers synthesized in this study and for established polymers with high electric field and/or high temperature stability.[6,14,35] (d) Electronic density of states for POFNBs and well-established dielectric polymers.

commercial high temperature polymers all reveal a dramatically increased ICC even at a much lower electric field, indicating a nonlinearly increasing electrical conduction as electric field magnitude increases. Polyether ether ketone (PEEK) has the largest bandgap among commercial high temperature polymers, while at 150 °C the ICC is still much higher than
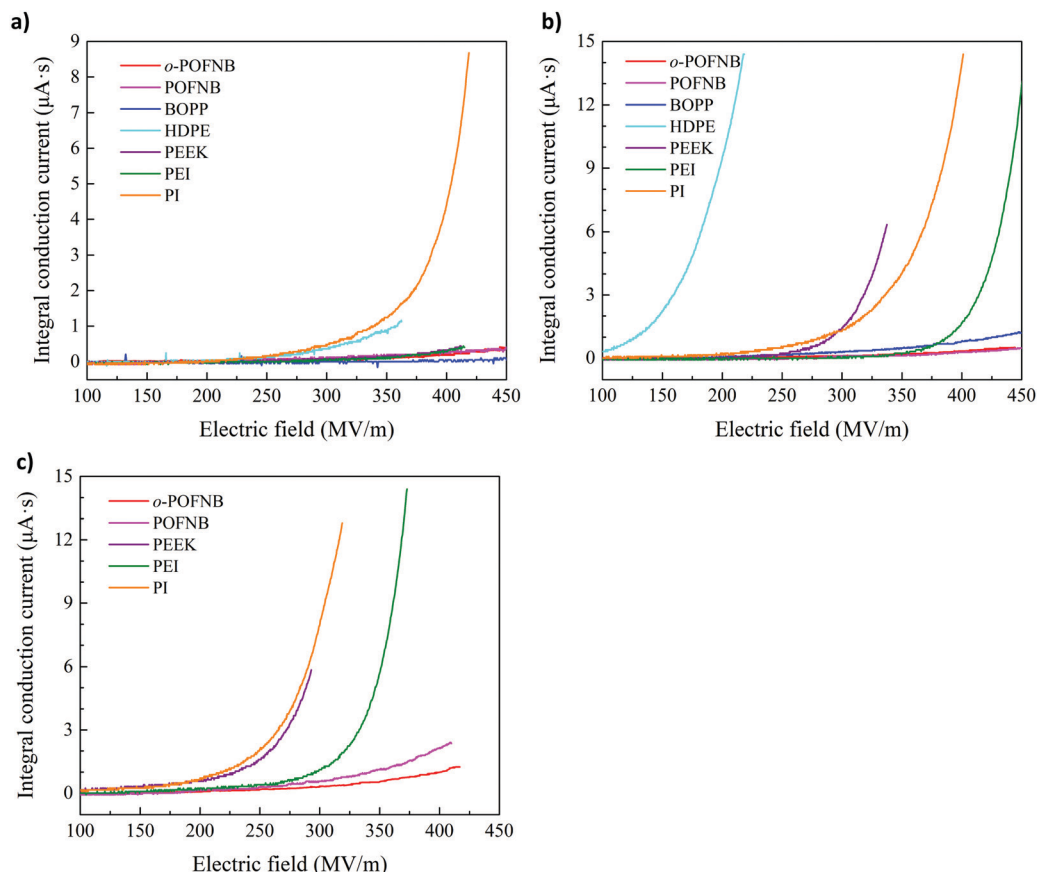
Fig. 2 High electric field conduction. Integral conduction current of o-POFNB and established dielectric polymers at (a) 25 °C (b) 100 °C (c) 150 °C.

that of polyetherimide (PEI) due to the lower T_g of PEEK (149 °C). At a concurrently high electric field and an elevated temperature, charge carriers move by hopping between adjacent localized sites with increased kinetic energy assisted by thermal and field effects. A larger bandgap gives rise to higher energy barriers to charge carriers to overcome for the hopping transport process and the charge carriers move by means of tunneling rather than hopping, leading to suppressed electrical conduction. The largest bandgap coupled with a higher T_g, imparts o-POFNB with the lowest high-field electrical conduction and best insulating properties at elevated temperatures.

Dielectric capacitors are key components in electrical and electronic systems, acting as energy storage and power converter input/output filtering due to their ultra-fast charge–discharge rate.[1,4,27] Advanced polymer dielectrics operable under not only electrical but also thermal extremes are highly desired for systems demanding high power density and payload efficiency. In energy storage capacitors, polymer dielectric films are placed between two metalized electrodes where energy is stored electrostatically upon application of the electric field. The energy density (U_e) for dielectric energy storage depends on the dielectric constant ε and applied electric field E according to the equation,[28–30] $U_e = 1/2\varepsilon\varepsilon_0 E^2$, where ε_0 is the vacuum permittivity. The capacitor efficiency illustrates the difference between total energy stored and total recoverable energy

released during the operation. It is clear that polymer's electric field endurance plays a crucial role in capacitors total energy density and efficiency.[14,20,25,31,32] Large bandgaps of POFNBs essentially gave rise to superior high electric field endurance.

The capacitive energy storage fundamentally stems from dielectric polarization, with the energy density proportional to the dielectric constant ε. Apart from the electrical conduction losses arising from the transport of charges, polarization is another key factor in determining the capacitor efficiency representing the energy loss originating from the re-orientation of dipoles. To provide evidence of the role that each functional group plays in the set of polymer structures, we performed Graph Neural Networks (GNN) based analysis to give more insight into the fundamental dielectric property-structure correlation. The contribution of different groups in the polymer structure is presented using the color coding of the local features learned using GNN (Fig. 3a). The dielectric constant and dissipation factor of POFNBs are shown in Fig. 3b and Fig. S25 (ESI†) following the rank of *meta*-Polyoxafluorinatednorbornene (m-POFNB) > o-POFNB > *para*-Polyoxafluorinatednorbornene (p-POFNB). As illustrated in Fig. 3a, the positions of the pendant –CF$_3$ group as well as the extent of rotation of the pedant benzene ring are integral in controlling the dielectric constant. The aromatic benzene ring in the polymer structure is attached to 'N' of the imide group in such a way that the lone pair of 'N' are in conjugation with imide oxygens, which does not allow cross conjugation between 'N'
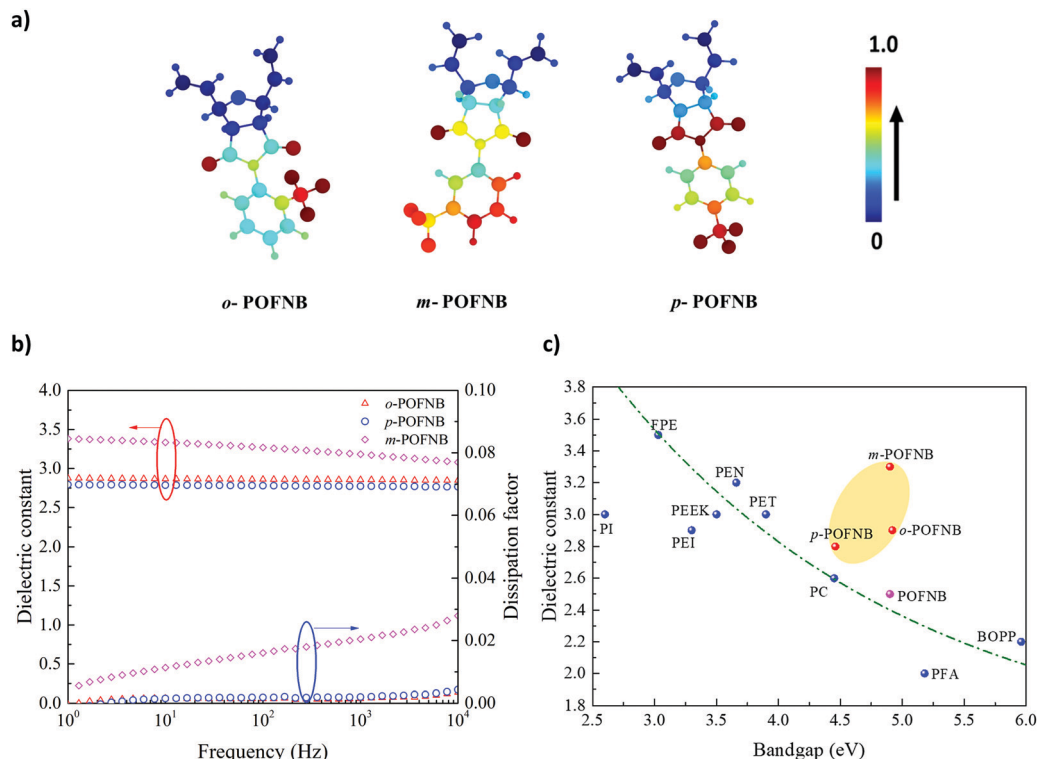
1310 | *Energy Environ. Sci.*, 2022, **15**, 1307–1314

This journal is © The Royal Society of Chemistry 2022

Fig. 3 Dielectric polarization. (a) Influence of each molecular fragment on the dielectric constant. (b) Dielectric constant and dielectric loss for o-POFNB, p-POFNB and m-POFNB. (c) Dielectric constants as a function of the bandgap for POFNBs and established dielectric polymers.

and benzene ring, avoiding possibility of having system with partial double bonds. This makes the flexible rotation of the –CF$_3$ attached benzene ring possible, and results in a stable dielectric constant with low loss. In the case of o-POFNB, the rotation of pendant benzene rings is restricted in comparison to p-POFNB and m-POFNB, which also contributes to the higher T_g of o-POFNB. These restrictions on dipole rotation cause relatively low dielectric constant compared to m-POFNB. The asymmetric position of –CF$_3$ in m-POFNB leads to enhanced dipolar polarization which results in increase in dielectric constant.[33] Although, in the case of p-POFNB, free rotation of the pedant group is available but the symmetric position of –CF$_3$ results in a lower dipole moment in total, leading to lower dielectric constant relative to m-POFNB and o-POFNB.[34] It has been demonstrated that the electronic part of the dielectric constant reveals an inverse relationship with the bandgap.[14] Close attention should be paid to bandgaps in the design of dielectric polymers. Dielectric constants at 100 Hz and RT as a function of the bandgap are shown in Fig. 3c. An evident inverse relationship can be observed between dielectric constants and bandgaps for most commercial and previously reported polymers, but the data points of POFNBs in this work appear to be outliers. The high operational electric fields and high dielectric constants of POFNBs can contribute to a higher energy density.

To reveal the high field energy storage performance, the dielectric displacement-electric field (DE) loop of o-POFNB was performed under ambient and elevated temperatures (Fig. 4a and Fig. S26–S33, ESI†). The narrow region between charging and discharging cycle of the DE loop indicates low energy loss.

Discharged energy density and efficiency were calculated using the DE loops (Fig. S26S33, ESI†). For o-POFNB at RT, the maximum discharged energy density is 10.4 J cc^{-1} with an efficiency of >92%, the highest among the whole set of polymers, due to the highest electric field endurance. At 150 and 200 °C the maximum discharged energy density values for o-POFNB are 8.3 J cc^{-1} and 6.5 J cc^{-1}, respectively (Fig. 4a and b). The temperature dependence of the discharged energy density of POFNBs and established commercial dielectric polymers is illustrated in Fig. 4c. POFNBs exhibit a stably high discharged energy density from RT to elevated temperatures in comparison to established dielectric polymers. Fig. 4d and e illustrated the discharged energy density and electric field endurance at 150 °C and 200 °C for POFNBs, established commercial dielectric polymers, and best reported polymers or polymer composites. At 150 °C, the discharged energy density of commercially available polymers is <1.5 J cm^{-3} (Fig. 4d). Efforts based on polymer composites with large bandgap fillers/coatings, or crosslinking modification of polymers elevate the energy density to the range of 2–5 J cm^{-3} (Fig. 4d). The POFNBs, with an intrinsically large bandgap and high T_g, exhibited significantly higher energy density and electric field endurance. o-POFNB possesses almost twice the upper limit of reported energy density. At 200 °C, most (∼70%) of the polymers and polymer composites in Fig. 4d could not withstand high electric fields and/or high temperatures. At such harsh conditions, the energy density of o-POFNB is still twice the upper limit of the reported energy density values
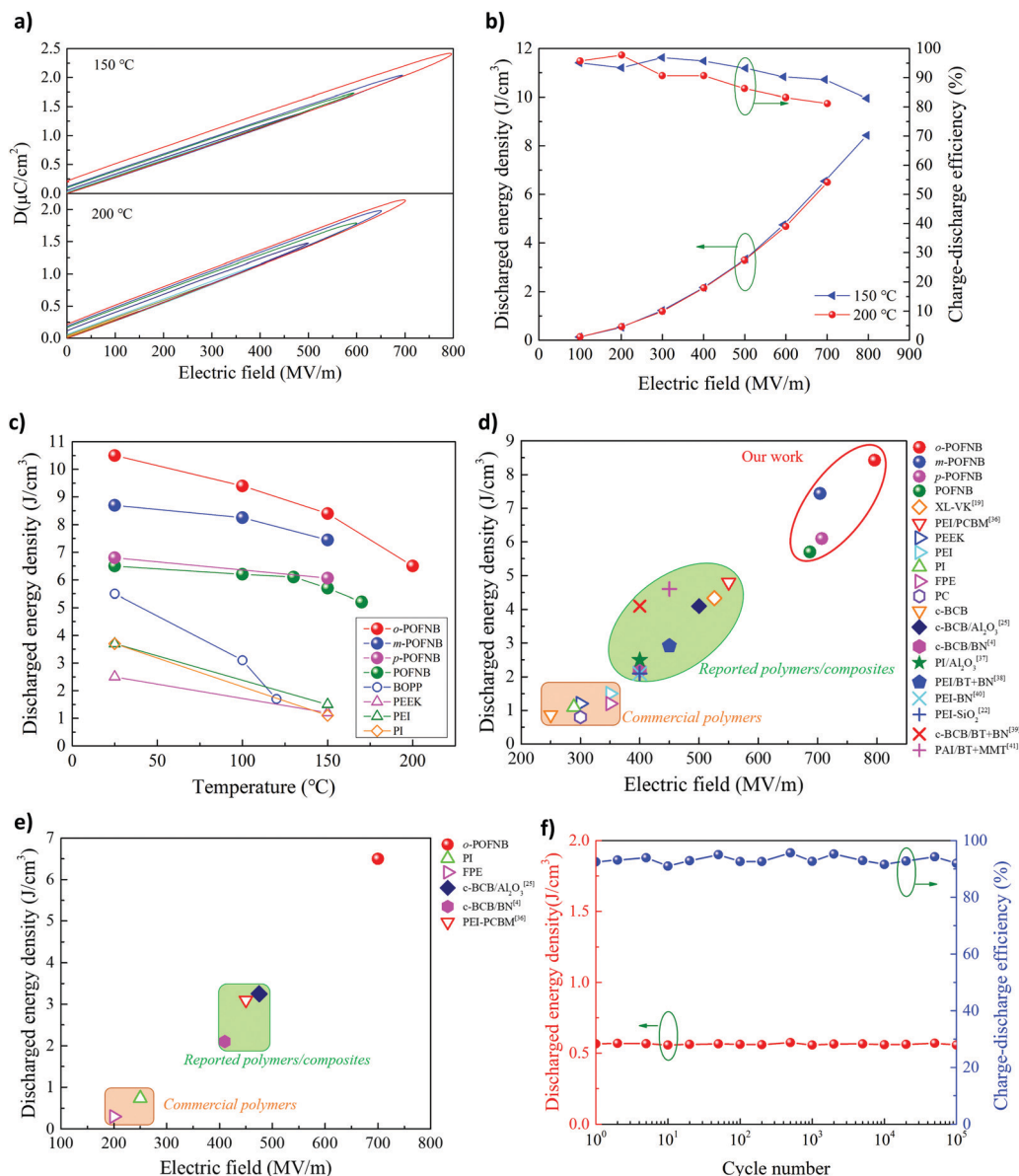
Paper

Fig. 4 High electric field energy storage. (a) Electric displacement- electric field loop (DE loop) and (b) energy storage performance of *o*-POFNB at 150 °C and 200 °C. (c) Discharged energy density and efficiency of POFNBs and well-established dielectrics as a function of the temperature. Discharged energy density and electric field endurance for POFNBs, established or reported dielectrics at (d) 150 °C and (e) 200 °C.[4,19,22,25,36–41] (f) Aging performance of *o*-POFNB at 200 °C and 200 MV m^{-1}.

(Fig. 4e). *o*-POFNB exhibits stable discharged energy density and high efficiency of > 91% under 200 MV m^{-1} (the operation electric field of BOPP) and 200 °C after 100 thousand of cyclic charging and discharging (Fig. 4f).

In summary, a novel polymer design strategy is developed where both high electric field and high temperature stability are achieved simultaneously. Wide bandgap, freely rotatable structural groups along with a combination of flexible and rigid moieties, achieved through a molecular engineering approach and verified using computational methods resulted in a class of polymer dielectrics with the highest ever discharged energy density up to 200 °C. All-organic polymers here exhibit flexibility and ease of processing, which makes them adaptable to a large number of electrical and electronic applications that operate in electrical and thermal extremes. The design strategy to develop all organic materials will pave the way for the development of future materials where stability at electrical and thermal extremes is needed.

Methods

1. Materials

Exo-3,6-epoxy-1,2,3,6-tetrahydrophthalic anhydride (≥98%) was purchased from TCI chemicals. Aniline (ACS reagent, ≥99.5%), 2-(trifluoromethyl)aniline (99%), 3-(trifluoromethyl)aniline (≥99%),

1312 | *Energy Environ. Sci.*, 2022, **15**, 1307–1314

This journal is © The Royal Society of Chemistry 2022

4-(trifluoromethyl)aniline (99%), sodium acetate (CH_3COONa, anhydrous, ReagentPlus®, ≥99.0%), and acetic anhydride (($CH_3CO)_2O$, ReagentPlus®, ≥99%) were purchased from Sigma Aldrich. Toluene (99.85%, anhydrous) was purchased from ACROS Organics. Hexane (Certified, H291-20); methylene chloride (Certified ACS, D37-20); pentane (Certified, 04062-20), sodium bicarbonate (Certified ACS, S233-3), and Celite 545 filter aid (Not acid washed powder, C212-25LB) were purchased from Fisher Scientific. Magnesium sulfate, $MgSO_4$ (anhydrous powder) was purchased from Oakwood Chemical. Grubbs Catalyst® 2nd Generation was purchased from Sigma Aldrich. Ethyl vinyl ether and methanol were purchased from Fisher Scientific.

2. Material characterization

^1H and ^{19}F NMR characterization for polymers and monomers was carried out using Bruker AVANCE 500 MHz spectrometer with TMS as an internal standard. Differential scanning calorimetry for T_g measurement was carried out using TA Instruments DSC Q-100 differential scanning calorimeter with heating and cooling rate of 10 °C min^{-1}. TA instruments TGA Q-500 was used to perform thermogravimetric analysis with heating rate of 20 °C min^{-1}. The molecular weight of the synthesized polymers is determined using Waters GPC system with dimethylacetamide (DMAc) as a mobile system and polystyrene as a standard. For polymer bandgap measurements, Agilent's 5000 UV/Vis/NIR spectrometer was used. Bruker D8 Quest Single Crystal Diffractometer with Cu micro source (1.542 Å) for wide angle X-Ray Diffraction analysis. It was equipped with a Photon-II detector (10 cm × 14 cm) to acquire 2D WAXS patterns.

3. Electrical characterization

Dielectric spectroscopy – the measurement was conducted using a Solartron SI 1260 frequency response analyzer with a Solartron 1296 dielectric interface. Gold/Palladium electrodes are sputter coated on both sides of the film with a diameter of 15 mm to ensure a good contact between electrodes and the film. High electric field conduction – the conduction at the high field was measured with a specially designed capacitive cancellation measurement system.[42] The system uses a dynamic negative feedback loop formed with a dual-phase lock-in amplifier to cancel the capacitive current throughout the measurement. The output signal represents the time-integrated conduction current (with a unit of 'μA s', the unit of the current 'μA' multiplying the unit of the time 's') across the sample, with accuracy for the small resistive current down to 10 ppm. High field displacement-electric field loop (DE loop) measurement – DE loop was employed using a modified Sawyer-Tower polarization loop tester with a unipolar positive half sinusoidal wave of 100 Hz. The measurement system consisted of a Trek Model 10/40 10 kV high voltage amplifier. Gold/palladium electrodes are coated on both sides of the film with a diameter of 3 mm using the sputter coating method to ensure a good contact between electrodes and the film.

4. DFT calculation

All density functional theory (DFT) calculations have been performed in VASP.[43] In the calculations, PI, o-POFNB, m-POFNB and p-POFNB were modeled using oligomers with 2 repeat units, given their complicated structures. For PP, the single-chain structure was applied. The physical structures of these polymers were relaxed using Perdew–Burke–Ernzerhof XC functional[44] and a plane-wave energy cutoff of 400 eV. The density of states was computed using the HSE06 functional.[45]

Author contributions

G. A. S. and Y. C. directed the research. A. D. and C. W. contributed equally to the experiments and manuscript preparation. A. D., O. Y., A. A., S. S. and J. V. synthesized the monomers and polymers and conducted the characterization experiments. C. W., Z. L., J. Z. and M. S. performed electrical experiments. A. M., P. R. and P. V. computed the contribution of different functional groups to the dielectric constants. Z. M. and M. C. conducted the Wide-Angle X-ray Scattering (WAXS) measurements. L. C. and R. R. conducted the electronic structure simulations. M. A. B. performed the SEM image analysis. A. D. and C. W. wrote the first manuscript and all authors participated in editing the manuscript.

Conflicts of interest

The authors declare no competing interests.

Acknowledgements

References

1 J. S. Ho and S. G. Greenbaum, Polymer Capacitor Dielectrics for High Temperature Applications, *ACS Appl. Mater. Interfaces*, 2018, **10**, 29189–29218.

2 J. Chen, X. Huang, B. Sun and P. Jiang, Highly Thermally Conductive Yet Electrically Insulating Polymer/Boron Nitride Nanosheets Nanocomposite Films for Improved Thermal Management Capability, *ACS Nano*, 2019, **13**, 337–345.

3 L. Zhang, H. Deng and Q. Fu, Recent progress on thermal conductive and electrical insulating polymer composites, *Compos. Commun.*, 2018, **8**, 74–82.

4 Q. Li, *et al.*, Flexible high-temperature dielectric materials from polymer nanocomposites, *Nature*, 2015, **523**, 576–579.

5 Y. Zhou and Q. Wang, Advanced polymer dielectrics for high temperature capacitive energy storage, *J. Appl. Phys.*, 2020, **127**, 240902.

6 C. Wu, *et al.*, Flexible Temperature-Invariant Polymer Dielectrics with Large Bandgap, *Adv. Mater.*, 2020, **2000499**, 1–6.

7 K. Yoshino, *et al.*, Novel properties of new type conducting and insulating polymers and their composites, *IEEE Trans. Dielectr. Electr. Insul.*, 1996, **3**, 331–344.

This journal is © The Royal Society of Chemistry 2022

Energy Environ. Sci., 2022, **15**, 1307–1314 | 1313

8 O. Bubnova, *et al.*, Semi-metallic polymers, *Nat. Mater.*, 2014, **13**, 190–194.

9 H. S. Sun, Y. C. Chiu and W. C. Chen, Renewable polymeric materials for electronic applications, *Polym. J.*, 2017, **49**, 61–73.

10 T. M. Swager, 50th Anniversary Perspective: Conducting/Semi-conducting Conjugated Polymers. A Personal Perspective on the Past and the Future, *Macromolecules*, 2017, **50**, 4867–4886.

11 Z. Bao and X. Chen, Flexible and Stretchable Devices, *Adv. Mater.*, 2016, **28**, 4177–4179.

12 M. leda, M. Nagao and M. Hikita, High-field Conduction and Breakdown in Insulating Polymers Present Situation and Future Prospects, *IEEE Trans. Dielectr. Electr. Insul.*, 1994, **1**, 934–945.

13 Y. Wang, *et al.*, Polymer-Based Gate Dielectrics for Organic Field-Effect Transistors, *Chem. Mater.*, 2019, **31**, 2212–2240.

14 V. Sharma, *et al.*, Rational design of all organic polymer dielectrics, *Nat. Commun.*, 2014, **5**, 1–8.

15 C. Wu, *et al.*, High Electric Field Conduction of Polymers at Ambient and Elevated Temperatures, *IEEE Conf. Electr. Insul. Dielectr. Phenom*, 2019, 486–489.

16 J. Ho and T. R. Jow, High Field Conduction in Heat Resistant Polymers at Elevated Temperature for Metallized Film Capacitors, *ACS Appl. Mater. Interfaces*, 2012, 399–402.

17 R. W. Johnson, J. L. Evans, P. Jacobsen, J. R. R. Thompson and M. Christopher, The Changing Automotive Environment: High-Temperature Electronics, *IEEE Trans. Electron. Packag. Manuf.*, 2004, **27**, 164–176.

18 C. Buttay, *et al.*, State of the art of high temperature power electronics, *Mater. Sci. Eng., B*, 2011, **176**, 283–288.

19 H. Li, *et al.*, Crosslinked fluoropolymers exhibiting superior high-temperature energy density and charge-discharge efficiency, *Energy Environ. Sci.*, 2020, **13**, 1279–1286.

20 L. Chen, *et al.*, Electronic Structure of Polymer Dielectrics: The Role of Chemical and Morphological Complexity, *Chem. Mater.*, 2018, **30**, 7699–7706.

21 K. Han, *et al.*, A Hybrid Material Approach Toward Solution-Processable Dielectrics Exhibiting Enhanced Breakdown Strength and High Energy Density, *Adv. Funct. Mater.*, 2015, **25**, 3505–3513.

22 Y. Zhou, *et al.*, A Scalable, High-Throughput, and Environmentally Benign Approach to Polymer Dielectrics Exhibiting Significantly Improved Capacitive Performance at High Temperatures, *Adv. Mater.*, 2018, **30**, 1–7.

23 G. H. Kim, *et al.*, High thermal conductivity in amorphous polymer blends by engineered interchain interactions, *Nat. Mater.*, 2015, **14**, 295–300.

24 D. Wang, *et al.*, Energy density issues of flexible energy storage devices, *Energy Storage Mater.*, 2020, **28**, 264–292.

25 H. Li, *et al.*, Scalable Polymer Nanocomposites with Record High-Temperature Capacitive Performance Enabled by Rationally Designed Nanostructured Inorganic Fillers, *Adv. Mater.*, 2019, **31**, 1–7.

26 Y. Thakur, M. H. Lean and Q. M. Zhang, Reducing conduction losses in high energy density polymer using nanocomposites, *Appl. Phys. Lett.*, 2017, **110**, 122905.

27 J. Ho and R. Jow, *Characterization of High Temperature Polymer Thin Films for Power Conditioning Capacitors*, 2009.

28 R. Ma, *et al.*, Rationally designed polyimides for high-energy density capacitor applications, *ACS Appl. Mater. Interfaces*, 2014, **6**, 10445–10451.

29 T. Zhang, *et al.*, A highly scalable dielectric metamaterial with superior capacitor performance over a broad temperature, *Sci. Adv.*, 2020, **6**, 1–8.

30 Z. Li, *et al.*, High energy density and high efficiency all-organic polymers with enhanced dipolar polarization, *J. Mater. Chem. A*, 2019, **7**, 15026–15030.

31 Y. Sun, S. A. Boggs and R. Ramprasad, The intrinsic electrical breakdown strength of insulators from first principles, *Appl. Phys. Lett.*, 2012, **101**, 132906.

32 L. Chen, T. D. Huan, Y. C. Quintero and R. Ramprasad, Charge injection barriers at metal/polyethylene interfaces, *J. Mater. Sci.*, 2015, **51**, 506–512.

33 C. Wu, *et al.*, Flexible cyclic-olefin with enhanced dipolar relaxation for harsh condition electrification, *Proc. Natl. Acad. Sci. U. S. A.*, 2021, **118**, e2115367118.

34 G. Hougham, G. Tesoro, A. Viehbeck and J. D. Chapple-Sokol, Polarization Effects of Fluorine on the Relative Permittivity in Polyimides, *Macromolecules*, 1994, **27**, 5964–5971.

35 A. Mannodi-Kanakkithodi, *et al.*, Rational Co-Design of Polymer Dielectrics for Energy Storage, *Adv. Mater.*, 2016, 6277–6291, DOI: 10.1002/adma.201600377.

36 C. Yuan, *et al.*, Polymer/molecular semiconductor all-organic composites for high-temperature dielectric energy storage, *Nat. Commun.*, 2020, **11**, 1–8.

37 D. Ai, *et al.*, Tuning Nanofillers in In Situ Prepared Polyimide Nanocomposites for High-Temperature Capacitive Energy Storage, *Adv. Energy Mater.*, 2020, **10**, 1–7.

38 H. Li, *et al.*, Ternary polymer nanocomposites with concurrently enhanced dielectric constant and breakdown strength for high-temperature electrostatic capacitors, *InfoMat*, 2020, **2**, 389–400.

39 Q. Li, *et al.*, Sandwich-structured polymer nanocomposites with high energy density and great charge–discharge efficiency at elevated temperatures, *Proc. Natl. Acad. Sci. U. S. A.*, 2016, **113**, 9995–10000.

40 A. Azizi, *et al.*, High-Performance Polymers Sandwiched with Chemical Vapor Deposited Hexagonal Boron Nitrides as Scalable High-Temperature Dielectric Materials, *Adv. Mater.*, 2017, **29**, 1–7.

41 Y. Wang, Z. Li, C. Wu and Y. Cao, High-temperature dielectric polymer nanocomposites with interposed montmorillonite nanosheets, *Chem. Eng. J.*, 2020, **401**, 126093.

42 Z. Li, C. Xu, H. Uehara, S. Boggs and Y. Cao, Transient characterization of extreme field conduction in dielectrics, *AIP Adv.*, 2016, **6**, 115025.

43 G. Kresse and J. Furthmüller, Efficient iterative schemes for ab initio total-energy calculations using a plane-wave basis set, *Phys. Rev. B: Condens. Matter Mater. Phys.*, 1996, **54**, 11169–11186.

44 J. P. Perdew, K. Burke and M. Ernzerhof, Generalized gradient approximation made simple, *Phys. Rev. Lett.*, 1996, **77**, 3865–3868.

45 J. Heyd, G. E. Scuseria and M. Ernzerhof, Hybrid functionals based on a screened Coulomb potential, *J. Chem. Phys.*, 2003, **118**, 8207–8215.

1314 | *Energy Environ. Sci.*, 2022, **15**, 1307–1314

This journal is © The Royal Society of Chemistry 2022